Eur. Phys. J. Plus (2015) **130**: 198
DOI 10.1140/epjp/i2015-15198-9

THE EUROPEAN PHYSICAL JOURNAL PLUS

Regular Article

Cosmological implications of dark energy model in DGP braneworld

Abdul Jawad[1,a] and Ines G. Salako[2,b]

[1] Department of Mathematics, COMSATS Institute of Information Technology, Lahore-54000, Pakistan
[2] Institut de Mathématiques et de Sciences Physiques (IMSP), 01 BP 613 Porto-Novo, Benin

Received: 11 July 2015 / Revised: 26 August 2015
Published online: 9 October 2015 –

Abstract. This paper is devoted to study the cosmic acceleration in the presence of pilgrim dark energy with conformal age of the universe in the framework of DGP braneworld. We explore different cosmological parameters such as Hubble, equation of state and squared speed of sound parameters. Also, we develop the $\omega_\vartheta - \omega'_\vartheta$. We observe that these parameters as well as plane provide consistent results with the observational data.

1 Introduction

It was confirmed through observational data that our universe undergoes accelerated expansion [1–3]. In order to explain this cosmic acceleration, two approaches have been adopted. One of them is the inclusion of some unknown element possessive repulsive force called dark energy (DE) in Einstein gravity. In this respect, the five-year WMAP data [4] provided the bounds $-1.11 < \omega_{DE} < -0.86$ (where ω_{DE} is the equation-of-state (EoS) parameter which is defined as the ratio of the pressure of the DE to its energy density). If $\omega_{DE} = -1$, then DE represents the cosmological constant which is the more favorable candidate for explanation of the accelerated expansion of the universe. In this scenario, the universe looks like asymptotically a de Sitter universe. In order to avoid the problems plagued with cosmological constant, different DE models have been developed, which include the family of chaplygin gas [5], holographic [6,7], new agegraphic [8], polytropic gas [9], pilgrim [10–12].

A second approach for understanding this strange component of the universe is the modified theories of gravity which are $f(R)$, $f(R,\mathcal{T})$ [13,14], $f(G)$ [15–17], where R is the curvature scalar, $\mathcal{T}$ the trace of the energy momentum tensor, G the invariant of Gauss-Bonnet defined as $G = R^2 - 4R_{\mu\nu}R^{\mu\nu} + R_{\mu\nu\lambda\sigma}R^{\mu\nu\lambda\sigma}$ and the theory so-called $f(T)$ gravity [18,19] as the modified version of the TEGR, where T denotes the torsion scalar. Special attention is attached to the so-called braneworld model proposed by Dvali, Gabadadze, and Porrati (DGP) [20–22] (for reviews, see [23]). In a cosmological scenario, this approach leads to a late-time acceleration as a result of the gravitational leakage from a 3-dimensional surface (3-brane) to a fifth extra dimension on Hubble distances.

More precisely this model presents two phases, of which one is accelerated but with an effective dark energy component with $w_{DE} > -1$, and dependent of the redshift. Hirano and Komiya [24] have generalized the modified Friedmann equation suggested by Dvali and Turner [25], for the purpose of achieving the phantom-like gap with an effective energy density with an EoS with $w < -1$. The DGP model presents two branches of solutions, *i.e.* the self-accelerating branch and the normal one. The self-accelerating branch leads to an accelerating universe without using any exotic fluid, but shows problems like ghost [26]. The normal branch need a dark energy component which is compatible with the observational data [27,28]. The extension of these models on the brane have been studied by in $f(R)$ gravity in order to obtain a self-acceleration in the normal branch [29]. The attempts of solutions for a DGP brane-world cosmology with a k-essence field were found in [30] showing big rip scenarios and asymptotically de Sitter phase in the future.

Moreover, it has also been shown, through the analysis of cosmological perturbations, that the DGP model contains a ghost mode [31–33]. Some authors pointed out a significantly worse fit to supernova data and the distance to the last-scattering surface in the pure DGP model as compared to the ΛCDM model [34]. Some have also tried to constrain

[a] e-mail: abduljawad@ciitlahore.edu.pk
[b] e-mail: ines.salako@imsp-uac.org

the DGP model using SNIa data and the baryon acoustic peak in the Sloan Digital Sky Survey and found similar results [35,36]. It has been suggested that the flat DGP model can be consistent with the SNIa data, it is under strong observational pressure by adding the data of the BAO and the CMB shift parameter. The open DGP model gives a slightly better fit relative to the flat model [37,38]. In general, it has been observed that the DGP model is disfavored by the joint observational constraints from SNIa, BAO, and CMB [34–38]. Recently, some observational efforts have been made DGP models and claimed that this model favors the observational data [39]. However, more attention has been required for removing the drawback of DGP scenario.

The holographic DE (HDE) has become an attractive DE model, nowadays, which is developed in the context of quantum gravity and widely used in solving the cosmological problems, by using the holographic principle, which stipulates that *the number of degrees of freedom of a physical system should scale with its bounding area rather than its volume* [40]. A relationship between ultraviolet and infrared (IR) cutoffs has been proposed by suggesting that the size of a system should not exceed the mass of a black hole (BH) of the same size [41]. By using this relationship, Li [7] developed the HDE density as follows:

$$\rho_\Lambda = 3n^2 M_p^2 L^{-2},$$

where n, M_p, L indicate the HDE constant, the reduced Planck constant, the IR cutoff, respectively. Compatibility of results [42–44] with the observational data has allowed to retain the different IR cutoffs: Hubble, particle, event horizons, conformal age of the universe, Ricci scalar, Granda-Oliveros, higher derivative of Hubble parameter, etc.

According to Cohen *et al.* [41], the bound of energy density from the idea of formation of BH in quantum gravity. However, it is suggested that formation of BH can be avoided through appropriate repulsive force, which resists the matter collapse phenomenon. This force can only provide phantom DE in spite of other phases of DE, like vacuum and quintessence DE. By keeping in mind this phenomenon, Wei [10] has suggested the DE model called pilgrim DE (PDE) on the speculation that phantom DE possesses a large negative pressure as compared to the quintessence DE, which helps violating the null energy condition and possibly prevent the formation of BH. In the past, many applications of phantom DE were present in the literature. For instance, phantom DE also plays an important role in the wormhole physics where the event horizon can be avoided due to its presence [45].

This motivated Wei [10] to develope the PDE model, and he analyzed this model with the Hubble horizon through different theoretical as well as observational aspects. Also, Saridakis *et al.* [46–55] have widely discussed the crossing of the phantom divide line, quintom as well as phantom-like nature of the universe in different frameworks and found interesting results in this respect. Recently, we have investigated this model by taking different IR cutoffs in flat as well as non-flat FRW universe with different cosmological parameters as well as cosmological planes [11,12]. This model has also been investigated in different modified gravities [56–64].

In the present paper, we check the role of PDE with the conformal age of the universe in the DGP braneworld. We develop different cosmological parameters and planes. The paper is organized as follows. In sect. 2, we present the generality of the DGP braneworld model. The basic cosmological parameters are presented in sect. 3. In the sect. 4, we develop the cosmological plane. The concluding remarks are presented in the last section.

2 DGP braneworld scenario

In the DGP braneworld framework, the field equation corresponding to non-flat FRW metric in the presence of PDE and CDM is given by [65,66]

$$H^2 - \frac{\epsilon}{r_c}\sqrt{H^2 + \frac{k}{a^2}} = \rho_m + \rho_\vartheta - \frac{3k}{a^2}\,, \tag{1}$$

where, a, $H = \frac{\dot{a}}{a}$ and k are the cosmic scale factor, the Hubble parameter and the spatial curvature, respectively. Also, $k = -1, 0, 1$ shows the open, flat and closed universes, respectively. Moreover, ρ_m and ρ_ϑ are the energy densities corresponding to CDM and PDE.

Here, we only consider $\epsilon = -1$, where the accelerating expansion of the universe can only be explained through the inclusion of the DE component in this scenario. In the present work, we consider a flat universe,

$$H^2 - \frac{\epsilon}{r_c}H = \rho_m + \rho_\vartheta, \tag{2}$$

which is suggested by Planck results [67]. There exist two different branches for the DGP model depending on the sign of ϵ. For $\epsilon = +1$, there is a de Sitter solution for eq. (2), with constant Hubble parameter, *i.e.*,

$$H = \frac{1}{r_c} \Rightarrow a(t) = a_0 e^{\frac{t}{r_c}},$$

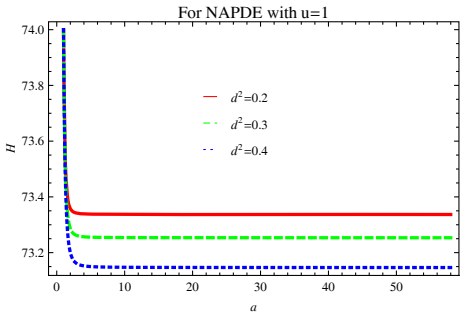

Fig. 1. Plot of H *versus* a for NAPDE in DGP with $u = 1$.

in the absence of any kind of energy or matter field on the brane (*i.e.*, $\rho = 0$).

In the present work, we consider $\epsilon = -1$, where the accelerating expansion of the universe can only be explained through the inclusion of the DE component in the DGP scenario. Thus, we start from eq. (2) and consider the interacting scenario of CDM (ρ_m) and PDE (ρ_ϑ). In the presence of interaction between PDE and CDM, the continuity equations take the following form:

$$\dot{\rho}_m + 3H\rho_m = \Theta, \quad \dot{\rho}_\vartheta + 3H(\rho_\vartheta + p_\vartheta) = -\Theta, \tag{3}$$

where Θ is the interaction term and possesses dynamical nature. The unknown nature of DE as well as CDM leads to the basic problem for the choice of interaction term. In the present scenario, we take the following form of interaction:

$$\Theta = 3d^2 H\rho_m, \tag{4}$$

where d^2 is an interacting constant and plays the role in exchanging the energy between the CDM and PDE components. Hence, eqs. (3) and (4) give

$$\rho_m = \rho_{m0} a^{3(d^2-1)}. \tag{5}$$

The PDE model is defined as follows:

$$\rho_\vartheta = 3n^2 m_p^{4-u} L^{-u}, \tag{6}$$

where u represents the PDE parameter. In this work, we discuss PDE by adopting the choice of the conformal age of the universe, which is defined as follows:

$$L = \eta = \int_0^t \frac{\mathrm{d}\tilde{t}}{a(\tilde{t})}. \tag{7}$$

Next, we explore the cosmological parameters as well as planes for three different values of u, *i.e.*, $u = 1, \ -1, \ -2$.

3 Basic cosmological parameters

The corresponding rate of change of PDE is

$$\dot{\rho}_\vartheta = -\frac{u\rho_\vartheta}{a}\left(\frac{H^2\Omega_\vartheta}{n^2 m_p^{2-u}}\right)^{\frac{1}{u}}. \tag{8}$$

The differential equation in terms of the Hubble parameter for the conformal age universe PDE becomes

$$\begin{aligned}\frac{\mathrm{d}H}{\mathrm{d}a} = {} & (aH)^{-1}((-((uH^2)a^{-1})(1-(\Omega_{m0}H_0^2 a^{3(d^2-1)}))H^{-2} - \epsilon(r_c H)^{-1}) \\ & \times ((H^2(1-(\Omega_{m0}H_0^2 a^{3(d^2-1)})H^{-2} - \epsilon(r_c H)^{-1}))n^{-2})^{(1/u)} + \Omega_{m0}H_0^2 \\ & \times a^{3(d^2-1)})(2H - \epsilon/r_c)^{-1}.\end{aligned} \tag{9}$$

The display of H *versus* a for three different values of d^2 is shown in figs. 1–3. For $u = 1$ (fig. 1), the Hubble parameter approaches $73.3^{+0.1}_{-0.1}$. However, it approaches $73.0010^{+0.0002}_{-0.0002}$ for the case $u = -1$ (fig. 2). For $u = -2$ (fig. 3), it approaches 74.012.

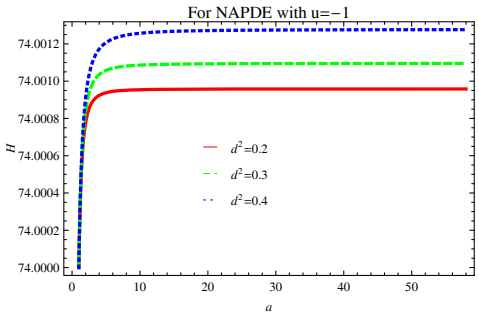

Fig. 2. Plot of H *versus* a for NAPDE in DGP with $u = -1$.

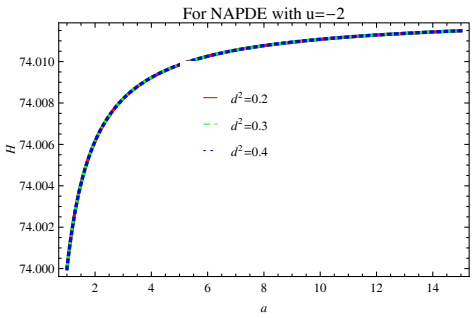

Fig. 3. Plot of H *versus* a for NAPDE in DGP with $u = -2$.

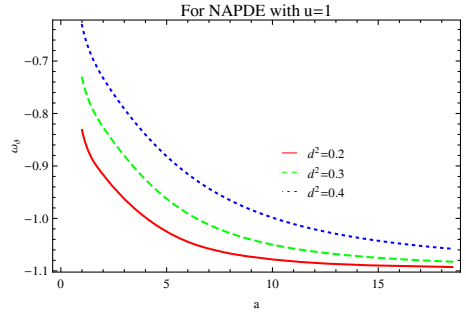

Fig. 4. Plot of ω_ϑ *versus* a for NAPDE in DGP with $u = 1$.

The evolution parameter corresponding to conformal age of the universe PDE has the form

$$\omega_\vartheta = -d^2(\Omega_{m0}H_0^2a^{3(d^2-1)}(H^2(1-(\Omega_{m0}H_0^2a^{3(d^2-1)})H^{-2}-\epsilon(r_cH)^{-1}))^{-1}) - u(3H)^{-1}((H^2(1-\Omega_{m0}H_0^2a^{3(d^2-1)}H^{-2}-\epsilon(r_cH)^{-1}))n^{-2})^{1/u}-1. \quad (10)$$

This EoS parameter is shown in figs. 4–6 *versus* the scale factor with same constant constraints as mentioned in the above sections. For $u = 1$ (fig. 4), it has been observed that the evolution parameter translates the universe from the quintessence-dominated phase towards the phantom-like phase of the universe by crossing the phantom divide line. Figure 5 shows that the EoS parameter has always remained in the quintessence phase of the universe for $d^2 = 0.4$. However, it crosses the phantom divide line from the phantom era to the quintessence era for $d^2 = 0.2,\ 0.3$. In the last case (fig. 6), the evolution parameter evolutes the universe in the phantom phase and also so close to vacuum DE region. It is also remarked that this model also favors the phantom crossing phenomenon as well as phantom universe which may help in avoiding the formation of BH in the universe.

For analyzing the stability of the NAPDE model, we use the squared speed of sound which is defined as follows:

$$\upsilon_s^2 = \frac{\dot{p_\vartheta}}{\dot{\rho_\vartheta}} = \frac{p'_\vartheta}{\rho'_\vartheta}, \quad (11)$$

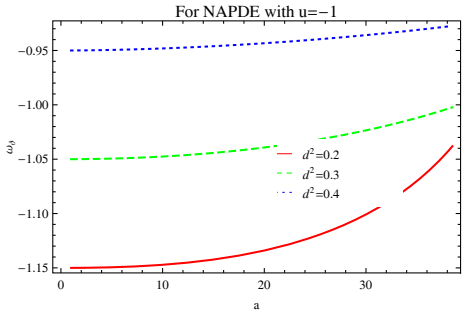

Fig. 5. Plot of ω_ϑ *versus* a for NAPDE in DGP with $u = -1$.

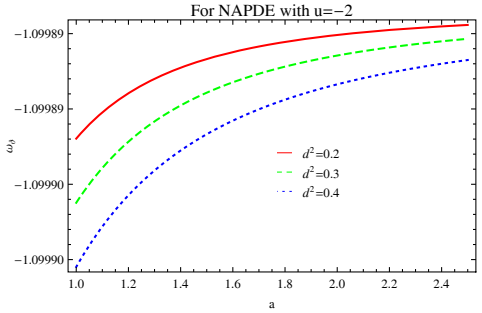

Fig. 6. Plot of ω_ϑ *versus* a for NAPDE in DGP with $u = -2$.

where pressure corresponds to PDE only. Differentiating the relation $p_\vartheta = \rho_\vartheta \omega_\vartheta$ with respect to $\ln a$ and dividing by ρ'_ϑ, we get

$$\frac{p'_\vartheta}{\rho'_\vartheta} = \omega_\vartheta + \frac{\rho_\vartheta}{\rho'_\vartheta}\omega'_\vartheta. \tag{12}$$

The squared speed of sound becomes

$$\begin{aligned} v_s^2 = 1 &- (u((-a^{-3+3d^2}\Omega_{m0}H_0^2 - (\epsilon H/r_c + H^2)n^{-2})^{1/u})(3H)^{-1} + (a^{3d^2} \\ &\times d^2 r_c \Omega_{m0} H_0^2)(a^{3d^2} r_c \Omega_{m0} H_0^2 + a^3 H(\epsilon - r_c H))^{-1} + (((-a^{-3+3d^2} \\ &\times \Omega_{m0}H_0^2 - (\epsilon H)/r_c + H^2)n^{-2})^{-1/u}(3a^{4+3d^2} d^2 r_c \Omega_{m0} H_0^2 H^2(-a^3 \\ &\times (-1+d^2)H^2(\epsilon - 2r_c H)(\epsilon - r_c H) + a^{3d^2} r_c \Omega_{m0} H_0^2(-\epsilon + 2r_c H)) \\ &+ u((-a^{-3+3d^2}\Omega_{m0}H_0^2 - (\epsilon H)/r_c + H^2)n^{-2})^{2/u}(a^{3d^2} r_c \Omega_{m0} H_0^2 + a^3 \\ &\times H(\epsilon - r_c H))^2(a^{3d^2} r_c \Omega_{m0} H_0^2 u - a^3 H(\epsilon - u\epsilon + r_c(-2+u)H) \\ &+ a^{1+3d^2} r_c \Omega_{m0} H_0^2((-a^{-3+3d^2}\Omega_{m0}H_0^2 - (\epsilon H)/r_c + H^2)n^{-2})^{1/u}(a^{3d^2} \\ &\times r_c \Omega_{m0} H_0^2 + a^3 H(\epsilon - r_c H))(a^{3d^2} r_c \Omega_{m0} H_0^2 u + a^2 H(a(-1+u)\epsilon \\ &+ H(-a r_c(-2+u) + a(-1+d^2)\epsilon - 3d^2 u\epsilon + 6r_c(-a(-1+d^2) \\ &+ d^2 u)H)))))(a^4 u H^3(\epsilon - 2r_c H)(a^(3d^2) r_c \Omega_{m0} H_0^2 + a^3 H(\epsilon - r_c H))^2)^{-1}. \end{aligned} \tag{13}$$

The plots of this squared speed of sound corresponding to the NAPDE model are displayed in figs. 7–9. It can be seen that the squared speed of sound shows positive behavior which leads to stability of the present model for all cases of u and d^2. Since the squared speed of sound remains greater than one (*i.e.*, $v_s^2 > 1$) [68], it exhibits superluminal behavior in all the cases of u and d^2 (figs. 7–9).

4 Cosmological plane

The ω_ϑ-ω'_ϑ plane (prime denotes the differentiation with respect to $x = \ln a$) also helps elaborating the accelerating expansion phenomenon [69]. Initially, this phenomenon was applied for analyzing the behavior of the quintessence

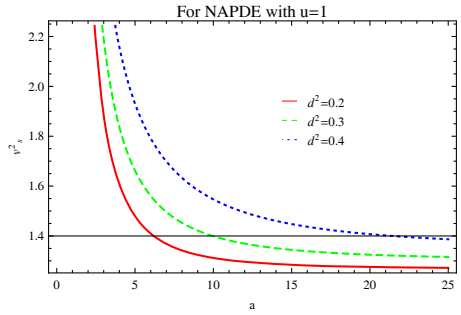

Fig. 7. Plot of v_s^2 *versus* a for NAPDE in DGP with $u = 1$.

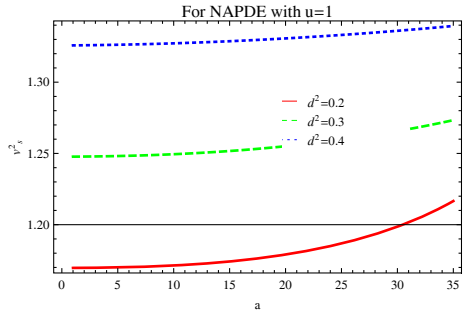

Fig. 8. Plot of v_s^2 *versus* a for NAPDE in DGP with $u = -1$.

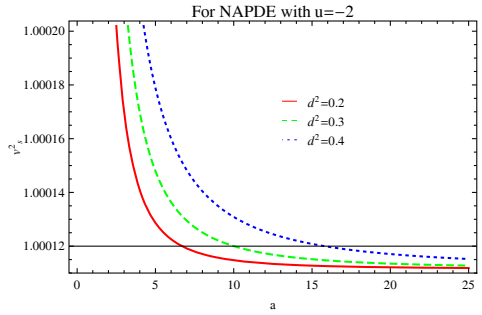

Fig. 9. Plot of v_s^2 *versus* a for NAPDE in DGP with $u = -2$.

model and it was found that the corresponding area occupied on the ω_ϑ-ω'_ϑ plane describes the thawing and freezing regions. The thawing models describe the region $\omega'_\vartheta > 0$, when $\omega_\vartheta < 0$, and the freezing models represent the region $\omega'_\vartheta < 0$, when $\omega_\vartheta < 0$. We also developed this plane for the present DE model by taking the derivative of ω_ϑ with respect to $x = \ln a$, by which one can get ω'_ϑ, for the NAPDE,

$$\begin{aligned}\omega'_\vartheta = &-a^{-1}(3a^{4+3d^2}d^2r_c\Omega_{m0}H_0^2H^2(-a^3(-1+d^2)H^2(\epsilon-2r_cH)(\epsilon-r_cH)\\
&+a^{3d^2}r_c\Omega_{m0}H_0^2(-\epsilon+2r_cH))+u((-a^{-3+3d^2}\Omega_{m0}H_0^2-(\epsilon H)/r_c+H^2)\\
&\times n^{-2})^{2/u}(a^{3d^2}r_c\Omega_{m0}H_0^2+a^3H(\epsilon-r_cH))^2(a^{3d^2}r_c\Omega_{m0}H_0^2u-a^3H(\epsilon\\
&-u\epsilon+r_c(-2+u)H))+a^{1+3d^2}r_c\Omega_{m0}H_0^2((-a^{-3+3d^2}\Omega_{m0}H_0^2-(\epsilon H)/r_c\\
&+H^2)n^{-2})^{1/u}(a^{3d^2}r_c\Omega_{m0}H_0^2+a^3H(\epsilon-r_cH))(a^{3d^2}r_c\Omega_{m0}H_0^2u+a^2\\
&\times H(a(-1+u)\epsilon+H(-ar_c(-2+u)+3a-1+d^2\epsilon-3d^2u\epsilon+6r_c\\
&\times(-a(-1+d^2)+d^2u)H))))/(3a^5H^3(\epsilon-2r_cH)(a^{3d^2}r_c\Omega_{m0}H_0^2+a^3\\
&\times H(\epsilon-r_cH))^2).\end{aligned} \tag{14}$$

The ω_ϑ-ω'_ϑ plane NAPDE model with different values of u in the DGP scenario is shown in figs. 10–12. For NAPDE, the cosmological plane only meets the thawing region for the cases of $u = -1,\ -2$, while it goes in the freezing region for $u = 1$ with all d^2 (figs. 10–12).

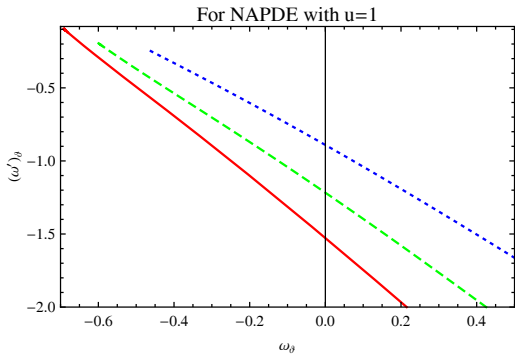

Fig. 10. Plot of ω_ϑ-ω'_ϑ *versus* a for NAPDE in DGP with $u = 1$.

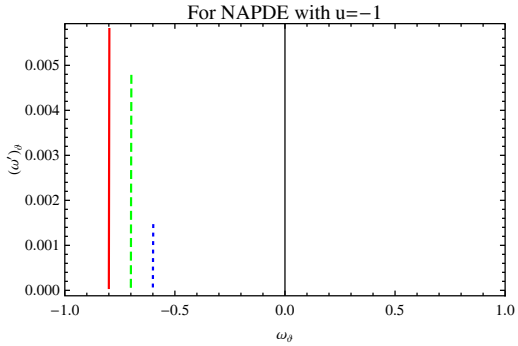

Fig. 11. Plot of ω_ϑ-ω'_ϑ *versus* a for NAPDE in DGP with $u = -1$.

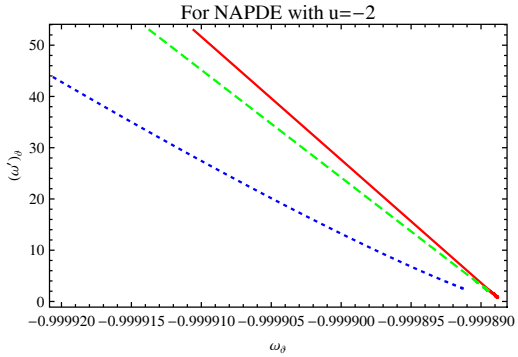

Fig. 12. Plot of ω_ϑ-ω'_ϑ *versus* a for NAPDE in DGP with $u = -2$.

5 Concluding remarks

We have investigated interacting PDE with the conformal age of the universe horizon, so-called NAPDE, in the DGP braneworld. The primary motivation for this paper is to analyze the cosmological scenario as well as the construction of possible constraints of the PDE parameter, u, where it fulfills the PDE phenomenon. In this connection, we have constructed the Hubble parameter, EoS parameter, squared speed of sound and ω_ϑ-ω'_ϑ, numerically. We have discussed these parameters corresponding to three values of $u = 1, -1, -2$ and three values of $d^2 = 0.2,\ 0.3,\ 0.4$. We have observed that the trajectories of the Hubble parameter $H(a)$ for $u = 1$ (fig. 1) approach $73.3^{+0.1}_{-0.1}$. However, they approach $73.0010^{+0.0002}_{-0.0002}$ for the case $u = -1$ (fig. 2). For $u = -2$ (fig. 3), they approach 74.012. This obtained range of $H(a)$ shows consistency with the observational data such as $H_0 = 73.8 \pm 2.4$ [70] and $H_0 = 74.3 \pm 1.5$ [71].

Also, the EoS parameter *versus* the scale factor was shown in figs. 4–6. For $u = 1$ (fig. 4), it has been observed that the evolution parameter translates the universe from quintessence-dominated phase towards phantom-like phase of the universe by crossing the phantom divide line. Figure 5 shows that the EoS parameter has always remained in the quintessence phase of the universe for $d^2 = 0.4$. However, it crosses the phantom divide line from phantom era to quintessence era for $d^2 = 0.2,\ 0.3$. In the last case (fig. 6), the evolution parameter evolutes the universe in the

Table 1. Summary of the observational data on ω_D.

ω_{D0}	Observational schemes	References
$-1.13^{+0.24}_{-0.25}$	Planck+WP+BAO	[67]
-1.09 ± 0.17	Planck+WP+Union 2.1	[67]
$-1.13^{+0.13}_{-0.14}$	Planck+WP+SNLS	[67]
$-1.24^{+0.18}_{-0.19}$	WMAP+eCMB+BAO+H_0+SNe Ia	[67]
$-1.073^{+0.090}_{-0.089}$	WMAP+eCMB+BAO+H_0	[72]
-1.084 ± 0.063	WMAP+eCMB+BAO+H_0+SNe	[72]

phantom phase and, also, is close to the vacuum DE region. It is also remarked that this model favors the phantom crossing phenomenon as well as phantom universe, which may help avoiding the formation of BH in the universe. It is also mentioned, here, that the ranges of the EoS parameter in the present scenario are consistent with the observational data (table 1).

We have also investigated the squared speed of sound corresponding to the NAPDE model, which has been displayed in figs. 7–9. It can be seen that the squared speed of sound shows positive behavior, which leads to stability of the present model for all cases of u and d^2. Since the squared speed of sound remains greater than one (*i.e.*, $\upsilon_s^2 > 1$) [68], it exhibits superluminal behavior in all the cases of u and d^2 (figs. 7–9). The ω_ϑ-ω'_ϑ plane NAPDE model with different values of u in DGP scenario is shown in figs. 10–12. For NAPDE, the cosmological plane only meets the thawing region for the cases of $u = -1, \ -2$, while it goes in the freezing region for $u = 1$, with all d^2, figs. 10–12.

IGS thanks IMSP for hospitality during the elaboration of this work.

References

1. A.G. Riess *et al.*, Astron. J. **116**, 1009 (1998).
2. S. Perlmutter *et al.*, Astrophys. J. **517**, 565 (1999).
3. T. Padmanabhan, Phys. Reps. **380**, 235 (2003).
4. WMAP Collaboration (E. Komatsu *et al.*), Astrophys. J. Suppl. **180**, 330 (2009).
5. A.Y. Kamenshchik, U. Moschella, V. Pasquier, Phys. Lett. B **511**, 265 (2001).
6. S.D.H. Hsu, Phys. Lett. B **594**, 13 (2004).
7. M. Li, Phys. Lett. B **603**, 1 (2004).
8. R.G. Cai, Phys. Lett. B **660**, 113 (2008).
9. K. Karami, S. Ghaffari, J. Fehri, Eur. Phys. J. C **64**, 85 (2009).
10. H. Wei, Class. Quantum Grav. **29**, 175008 (2012).
11. M. Sharif, A. Jawad, Eur. Phys. J. C **73**, 2382 (2013).
12. M. Sharif, A. Jawad, Eur. Phys. J. C **73**, 2600 (2013).
13. E.H. Baffou, A.V. Kpadonou, M.E. Rodrigues, M.J.S. Houndjo, J. Tossa, Astrophys. Space Sci. **355**, 2197 (2014).
14. M.J.S. Houndjo, Int. J. Mod. Phys. D. **21**, 1250003 (2012).
15. S.'I. Nojiri, S.D. Odintsov, Phys. Lett. B **631**, 1 (2005) S. Nojiri, S.D. Odintsov, A. Toporensky, P. Tretyakov, arXiv:0912.2488.
16. K. Bamba, S.D. Odintsov, L. Sebastiani, S. Zerbini, arXiv:0911.4390.
17. K. Bamba, C.-Q. Geng, S. Nojiri, S.D. Odintsov, arXiv:0909.4397.
18. K. Bamba, J. de Haro, S.D. Odintsov, JCAP **02**, 008 (2013).
19. M. Jamil, D. Momeni, R. Myrzakulov, Eur. Phys. J. C **72**, 2267 (2012).
20. G.R. Dvali, G. Gabadadze, M. Porrati, Phys. Lett. B **485**, 208 (2000).
21. C. Deffayet, Phys. Lett. B **502**, 199 (2001).
22. C. Deffayet, G.R. Dvali, G. Gabadadze, Phys. Rev. D **65**, 044023 (2002).
23. K. Koyama, Gen. Relativ. Gravit. **40**, 421 (2008).
24. K. Hirano, Z. Komiya, Gen. Relativ. Gravit. **42**, 2751 (2010).
25. G. Dvali, M.S. Turner, arXiv:astro-ph/0301510.
26. K. Koyama, Class. Quantum. Grav. **24**, R231 (2007).
27. A. Lue, G.D. Starkman, Phys. Rev. D **70**, 101501 (2004).
28. R. Lazkoz, R. Maartens, E. Majerotto, Phys. Rev. D **74**, 083510 (2006).
29. M. Bouhmadi-Lopez, JCAP **11**, 011 (2009).
30. M. Bouhmadi-Lopez, L. Chimento, Phys. Rev. D **82**, 103506 (2010).
31. A. Lue, R. Scoccimarro, G.D. Starkman, Phys. Rev. D **69**, 124015 (2004).

32. K. Koyama, R. Maartens, JCAP **01**, 016 (2006).
33. D. Gorbunov, K. Koyama, S. Sibiryakov, Phys. Rev. D **73**, 044016 (2006).
34. I. Sawicki, S.M. Carroll, arXiv:astro-ph/0510364.
35. M. Fairbairn, A. Goobar, Phys. Lett. B **642**, 432 (2006).
36. U. Alam, V. Sahni, Phys. Rev. D **73**, 084024 (2006).
37. R. Maartens, E. Majerotto, Phys. Rev. D **74**, 023004 (2006).
38. Y.S. Song, I. Sawicki, W. Hu, Phys. Rev. D **75**, 064003 (2007).
39. M. Sadegh Movahed, M. Farhang, S. Rahvar, Int. J. Theor. Phys. **48**, 1203 (2009).
40. L. Susskind, J. Math. Phys. **36**, 6377 (1995).
41. A. Cohen, D. Kaplan, A. Nelson, Phys. Rev. Lett. **82**, 4971 (1999).
42. M. Li, Phys. Lett. B **603**, 1 (2004).
43. H. Wei, R.G. Cai, Phys. Lett. B **660**, 113 (2008).
44. C. Gao, X. Chen, Y.G. Shen, Phys. Rev. D **79**, 043511 (2009).
45. M. Sharif, A. Jawad, Eur. Phys. J. Plus **129**, 15 (2014).
46. Y.-F. Cai *et al.*, Phys. Rep. **493**, 1 (2010).
47. E.N. Saridakis, Nucl. Phys. B **819**, 116 (2009).
48. G. Gupta, E.N. Saridakis, A.A. Sen, Phys. Rev. D **79**, 123013 (2009).
49. M.R. Setare, E.N. Saridakis, JCAP **03**, 002 (2009).
50. M.R. Setare, E.N. Saridakis, Phys. Lett. B **671**, 331 (2009).
51. E.N. Saridakis, P.F. Gonzalez-Diaz, C.L. Siguenza, Class. Quantum. Grav. **26**, 165003 (2009).
52. E.N. Saridakis, Phys. Lett. B **676**, 7 (2009).
53. E.N. Saridakis, Phys. Lett. B **660**, 138 (2008).
54. E.N. Saridakis, Phys. Lett. B **661**, 335 (2008).
55. M.R. Setare, E.N. Saridakis, Phys. Lett. B **671**, 331 (2009).
56. M. Sharif, S. Rani, J. Exp. Theor. Phys. **119**, 75 (2014).
57. S. Chattopadhyay, A. Jawad, D. Momeni, R. Myrzakulov, Astrophys. Space Sci. **353**, 279 (2014).
58. A. Jawad, S. Rani, Adv. High Ener. Phys. **2015**, 952156 (2015).
59. A. Jawad, Astrophy. Space Sci. **356**, 119 (2015).
60. A. Jawad, S. Rani, Astrophy. Space Sci. **357**, 88 (2015).
61. A. Jawad, Astrophy. Space Sci. **353**, 691 (2014).
62. A. Jawad, Eur. Phys. J. Plus **129**, 207 (2014).
63. A. Jawad, Eur. Phys. J. C **75**, 206 (2015).
64. A. Jawad, S. Rani, Adv. High Ener. Phys. **2015**, 259578 (2015).
65. K. Koyama, Gen. Relativ. Gravit. **40**, 421 (2008).
66. M. Li, X. Li, S. Wang, Y. Wang, Commun. Theor. Phys. **56**, 525 (2011).
67. P.A.R. Ade *et al.*, arXiv:1303.5076.
68. R. Garca-Salcedo, T. Gonzalez, I. Quiros, Phys. Rev. D **89**, 084047 (2014).
69. R.R. Caldwell, E.V. Linder, Phys. Rev. Lett. **95**, 141301 (2005).
70. A.G. Riess *et al.*, Astrophys. J. **730**, 119 (2011).
71. W.L. Freedman *et al.*, Astrophys. J. **758**, 24 (2012).
72. G.F. Hinshaw *et al.*, Astrophys. J. Suppl. **208**, 19 (2013).